

Self-defocusing of converging laser beams

Yu. K. Danileiko, L. M. Degtyarev, A. L. Kopa-Ovdienco, and T. P. Lebedeva

Institute of General Physics, Academy of Sciences of the USSR

(Submitted 28 December 1983)

Zh. Eksp. Teor. Fiz. **87**, 730–740 (September 1984)

Self-defocusing in sharply focused laser beams is investigated. The analysis is valid for thermal defocusing and defocusing due to the presence of free carriers generated during multiphoton ionization by the incident light. Stationary and nonstationary self-defocusing are examined for different nonlinearities of the medium. The effect of nonlinear absorption on the process under investigation is determined in the stationary case. It is found that the maximum change in the permittivity of the medium, in both stationary and nonstationary advanced self-defocusing, is independent of the frequency of incident radiation and is determined by the square of the focusing angle. Intensity saturation occurs in the region of the nonlinear focus for stationary self-defocusing. For nonstationary defocusing, the pulse of transmitted radiation is cut off, and the maximum intensity in the focus is determined by the nature of the nonlinearity of the medium and the slope of the leading edge of the incident-radiation pulse. The change in the divergence of the beam in the case of sharp focusing in a nonlinear medium is elucidated, and the feasibility of experimental observation of the phenomenon is analyzed. Comparison of numerical calculations with the solution obtained in the aberration-free approximation is used as a basis for a discussion of the range of validity of this approximation for this class of problems.

1. INTRODUCTION AND FORMULATION OF THE PROBLEM

Self-defocusing of light is among well-known phenomena in the physics of interaction between powerful laser radiation and matter. It is interesting in itself, from the standpoint of nonlinear optics, and because self-defocusing can modify the process of interaction between laser radiation and matter.

Most publications have examined the effect of defocusing on the propagation of a collimated laser beam (see, for example, Refs. 1–5). However, studies of these interaction processes frequently employ high light intensities produced by sharp focusing. Self-defocusing is therefore of particular interest in the case of sharply focused beams.

Interaction processes that may be accompanied by a reduction in the refractive index of the medium include multiphoton ionization, heating resulting from laser absorption, laser thermochemistry, and so on. Since each type of interaction is characterized by its own variation of the refractive index of the nonlinear medium, it is interesting to examine common features of self-defocusing for different types of nonlinearity of the medium. This question has not been examined in the literature although there are some individual publications in which particular cases are investigated numerically.⁶

The aim of this paper was to determine the light-field characteristics of the interaction region such as maximum intensity and energy density, the space-time dynamics of the transmitted pulse, as well as their dependence on the type of nonlinearity and focusing conditions.

The propagation of a powerful light beam in a nonlinear medium will be discussed in terms of the well-known parabolic equation for the electric field E of an electromagnetic wave propagating in the z direction:

$$2ik \frac{\partial E}{\partial z} + \Delta_r E + k^2 \frac{\delta \epsilon(|E|)}{\epsilon_0} E = 0, \quad (1)$$

where k is the wave number, $\epsilon = \epsilon_0 + \delta \epsilon(|E|)$ is the permittivity of the medium, and $\delta \epsilon \ll \epsilon_0$. The nonlinear part $\delta \epsilon$ is determined by the type of interaction between the field and the medium. For example, if the self-defocusing process is due to the presence of free carriers generated by multiphoton ionization by light, the behavior of the real part of $\delta \epsilon$ is described by

$$\frac{d\delta \epsilon}{dt} = \frac{\alpha_n}{n\hbar\omega} \beta |E|^{2n} - \frac{\delta \epsilon}{\tau}, \quad (2)$$

where α_n is the coefficient of n -photon ionization by a photon of energy $\hbar\omega$, β is a constant governing the connection between the real part of $\delta \epsilon$ and the density of nonequilibrium carriers, and τ is the nonlinearity relaxation time.

It is important to note that nonstationary thermal self-defocusing can also be examined on the basis of (2) when $1/\tau = 0$.

2. STATIONARY SELF-DEFOCUSING

Consider the self-defocusing process for short nonlinearity relaxation times $\tau \ll \tau_p$, where τ_p is the incident-pulse length (stationary case). We may then write

$$\delta \epsilon = \epsilon_m |E|^m. \quad (3)$$

To elucidate the qualitative features of the process, consider the behavior of a focused Gaussian beam in the so-called aberration-free approximation⁷ in the absence of absorption. To this end substitute $E = A \exp(-ikS)$ and consider the set of equations for the amplitude A and phase S of the field. Following Ref. 7, we shall seek A and S in the form

$$A = \frac{E_0}{f(z)} \exp \left\{ -\frac{r^2}{2a_0^2 f^2(z)} \right\}, \quad S = \frac{r^2}{2} \beta(z) + \varphi(z). \quad (4)$$

The initial conditions for the basic problem are: $f(0) = 1$, $\beta(0) = 1/R$, where R is the radius of curvature of the wave front at entry to the nonlinear medium and a_0 is the initial width of the Gaussian beam.

Using (4), we find from (1) and (3) that the dimensionless width $f(z)$ of the beam is the solution of the equation

$$\left(\frac{\partial f}{\partial z} \right)^2 = \frac{1}{k^2 a_0^4} \left(1 - \frac{1}{f^2} \right) + \frac{\epsilon_m}{\epsilon_0 a_0^2} E_0^m \left(\frac{1}{f^m} - 1 \right) + \frac{1}{R^2}. \quad (5)$$

The maximum light intensity is determined from (5) as the value of f for which $\partial f / \partial z = 0$.

We now define the defocusing threshold as the condition under which the maximum intensity on the caustic is reduced by a factor of two as compared with the linear problem, i.e.,

$$1/f_c^2 = 0,5 (l_d/R)^2, \quad (6)$$

where $l_d = ka_0^2$ is the diffraction length of the incident beam. Substituting $\partial f / \partial z = 0$ in (5), we then obtain the threshold (critical) value $\delta\epsilon_{\text{crit}}$ at entry to the medium:

$$\frac{\delta\epsilon_{\text{crit}}}{\epsilon_0} = \frac{\epsilon_m E_0^m}{\epsilon_0} = -\frac{2^{m/2}}{2} (ka_0)^{-2} \left(\frac{l_d}{R} \right)^{2-m}. \quad (7)$$

Analysis of (5) shows that, in the highly nonlinear region (well above the threshold), the light intensity in the focal region ceases to increase with increasing incident intensity, and there is merely a broadening of the beam. The field amplitude in the focal region, and the corresponding nonlinear permittivity of the medium under the conditions of saturation, are given by

$$\frac{\epsilon_m}{\epsilon_0} |E_{\text{max}}|^m = \frac{\epsilon_m}{\epsilon_0} E_0^m - \frac{a_0^2}{R^2}$$

or

$$\frac{\delta\epsilon_{\text{max}}}{\epsilon_0} = \frac{\delta\epsilon(0)}{\epsilon_0} - \frac{a_0^2}{R^2}. \quad (8)$$

The resulting expression $\Delta n \sim (a_0/R)^2$ has a simple physical interpretation. It is a reflection of the fact that the intensity at the focus decreases when the nonlinear advance in phase along the caustic becomes equal to $\pi/2$.

Let us now consider the variation in the divergence of the beam as it passes through the nonlinear medium. Equation (5) shows that the intensity distribution is completely symmetric with respect to the nonlinear focus ($\partial f / \partial z = 0$). Moreover, at large distances from the geometric focus ($f \gg 1$), the curvature of the phase front is $\partial f / \partial z \approx 1/R$, which shows that the variation in the divergence of the beam is small in comparison with linear optics.

3. STATIONARY SELF-DEFOCUSING. NUMERICAL CALCULATIONS

As a check on the predictions of the aberration-free approximation, we carried out a numerical solution of (1) and (3) for sharply-focused beams with an initial Gaussian intensity distribution over the cross section and different values of m . The numerical solution was based on the difference scheme proposed in Ref. 8. In the case of strong nonlinearity,

we used the scheme with viscosity (see, for example, Ref. 9).

Our calculations have shown that, even then the nonlinearity is slight, the numerical solution of (1) and (3) is qualitatively different from the solution obtained in the aberration-free approximation, just as in the case of self-focusing.^{10,11} To compare the numerical calculations with the aberration-free approximation, Figure 1 shows the self-defocusing threshold [see condition (6)] as a function of the nonlinearity index m . The threshold nonlinearity of the permittivity is normalized to $\delta\epsilon_{\text{crit}}$ given by (7). The calculations are shown for two values of l_d/R . It is clear from Fig. 1 that, when $m \geq 2$, the threshold nonlinear permittivity (in units of $\delta\epsilon_{\text{crit}}$) is not very dependent on the focusing conditions, i.e., on l_d/R . This is a consequence of the fact that the interaction is mostly confined to the region near the focus.

When the self-defocusing threshold is substantially exceeded, the maximum light intensity ceases to grow with increasing incident intensity (saturation effect) and we observe only broadening of the focal region, which confirms the basic conclusion of the aberration-free approximation. We note that, in the case of cubic nonlinearity, the nonlinear focus is shifted along the path of the ray. The variation in the radial distribution of intensity with z is shown in Fig. 2 for the cubic nonlinearity $\delta\epsilon(0,0) = 10^3 \delta\epsilon_{\text{crit}}$. It is clear that the radial distribution ceases to be Gaussian in the course of propagation, and the lateral intensity profile acquires a flat top with raised edges. For convenience, the intensity is expressed in terms of $\delta\epsilon(0,z)R^2/a_0^2$ and the distance to the geometric focus in units of the length l_c of the linear caustic. In terms of these variables, the above solution for sharply-focused beams is practically independent of the focusing angle and wavelength.

Calculations, performed for other cases of negative nonlinearity ($m = 1-4$) have shown that the type of nonlinearity does not modify the basic self-defocusing structure. In particular, it has been found that, whatever the degree of nonlinearity m in the focal region, the maximum intensity and maximum nonlinear part of the permittivity of the medi-

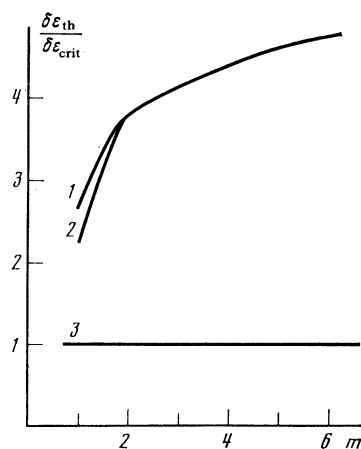


FIG. 1. Threshold value of nonlinear permittivity for stationary self-defocusing as a function of the nonlinearity exponent m . The numerical solution is shown for two values of l_d/R , namely, 30 (curve 1) and 300 (curve 2). For comparison, we also show the threshold in the aberration-free approximation (curve 3).

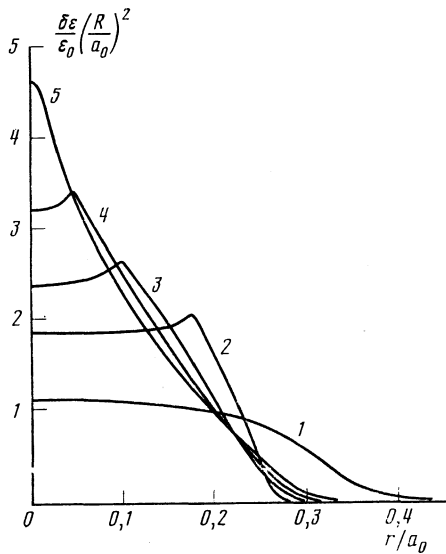


FIG. 2. Variation in the radial intensity distribution for the cubic nonlinearity when $\delta\epsilon(0, 0) = 10^3 \delta\epsilon_{\text{crit}}$ near the focus and $l_d/R = 100$. Curve 1: $R - z = -20l_c$; curve 2: $R - z = -8l_c$; curve 3: $R - z = -3l_c$; curve 4: $z = R$; curve 5: $R - z = 2.5l_c$.

um in the case of saturation are given by¹²

$$\frac{\delta\epsilon_{\text{max}}}{\epsilon_0} = \frac{\epsilon_m |E_{\text{max}}|^m}{\epsilon_0} \approx -5 \left(\frac{a_0}{R} \right)^2. \quad (9)$$

We have also investigated the effect of nonlinear absorption on self-defocusing. Absorption was introduced in (3) as follows: $\epsilon_m = \epsilon_m' + i\epsilon_m''$. Numerical calculations show that inclusion of absorption reduces the longitudinal size of the focal region, and a well-defined dip appears in the radial intensity distribution as the nonlinear focus is approached. However, the maximum intensity that can be achieved on the caustic is determined exclusively by the real part ϵ_m' [see (9)] and is not very dependent on the degree of absorption. The validity of this conclusion was checked against examples in which the total beam intensity behind the caustic fell by a factor of more than 100.

An important feature of the self-defocusing process is the variation in the phase characteristics of the wave due to the appearance of the induced negative lens in the medium. Numerical calculations have shown that, for sharp focusing of incident radiation, the wave front at the center of the caustic is nearly plane, and a considerable departure from the planar configuration (greater than $\lambda/4$) occurs only in the wings of the radial distribution, which contain no more than 10% of the beam energy. The presence of such a cross section with a plane phase front ensures that, when it is coincident with the exit surface of the nonlinear medium, a reduction is observed in the divergence of the beam, due to the increase in its diameter. This effect was first observed and explained qualitatively in Ref. 13.

However, when the focus is located deep in the medium, no change in the divergence of the beam is observed, and the radial field distribution well away from the caustic remains symmetric relative to the focal plane.¹⁾ The change in the optical characteristics of the nonlinear medium results only in an additional advance in the phase of the beam as a whole,

i.e., the nonlinear medium is then equivalent to a flat plate with a negative refractive index. Aberration of the phase profile at the exit from the nonlinear medium occurs only in the wings of the radial distribution, and has therefore no appreciable effect on beam propagation.

It follows from the foregoing that, when the focus lies deep inside the medium, the amplitude and phase distributions at the exit ($z \gtrsim 2R$) carry practically no information about the self-defocusing in the focal region. This information is carried only by the additional advance in phase $\Delta\varphi$. However, an appreciable value of $\Delta\varphi$ can be obtained only well above the threshold ($\Delta\varphi = 2\pi$ with $\delta\epsilon(0) \approx 158\epsilon_{\text{crit}}$).

4. NONSTATIONARY SELF-DEFOCUSING IN THE ABERRATION-FREE APPROXIMATION

We have examined above the basic feature of the self-focusing process for the instantaneous-type nonlinearity. However, the more usual situation is that where defocusing occurs in a medium in which nonlinearity accumulates in time. Examples include thermal defocusing, defocusing by free carriers during slow recombination $\tau \gg \tau_p$, and so on. Processes due to the nonlinear imaginary part of $\delta\epsilon$ were examined in Ref. 14.

Calculations performed for stationary defocusing have shown that the basic features of this process are qualitatively described by the aberration-free approximation. It follows that this approximation will probably also reproduce the basic features of self-interaction in the presence of accumulating nonlinearity $\delta\epsilon(t)$.

Consider the case where recombination can be neglected, i.e., $\tau \gg \tau_p$. The nonlinear part of the permittivity (2) is then given by

$$\delta\epsilon(t) = \epsilon_m \int_0^t E^m(t') dt'. \quad (10)$$

We now substitute

$$E = E_0 \sqrt{\varphi(t)} A \exp\left(-i \frac{l_d}{R} S\right), \quad (11)$$

where $\varphi(t)$ is the incident intensity pulse and E_0^2 is its peak value. The equations for the dimensionless amplitude A and phase S of the light-wave field can then be written in the following form:

$$\begin{aligned} \frac{\partial A}{\partial z} &= \frac{\partial A}{\partial r} \frac{\partial S}{\partial r} + \frac{A}{2} \left(\frac{1}{r} \frac{\partial S}{\partial r} + \frac{\partial^2 S}{\partial r^2} \right), \\ \frac{\partial S}{\partial z} &= \frac{1}{2} \left(\frac{\partial S}{\partial r} \right)^2 \\ &+ \frac{1}{(l_d/R)^2} \int_0^{(z)} A^m dx - \frac{1}{2A(l_d/R)^2} \left[\frac{1}{r} \frac{\partial A}{\partial r} + \frac{\partial^2 A}{\partial r^2} \right]. \end{aligned} \quad (12)$$

We have transformed here for convenience to dimensionless variables ($z \rightarrow z/R$, $r \rightarrow r/a_0$). In addition, since the time determines only the process of accumulation of $\delta\epsilon$, it is convenient to transform to the new coordinate

$$x(t) = \frac{\epsilon_m E_0^m}{\epsilon} (ka_0)^2 \int_0^t \varphi^{m/2}(t') dt',$$

which carries all the necessary information about the nonlin-

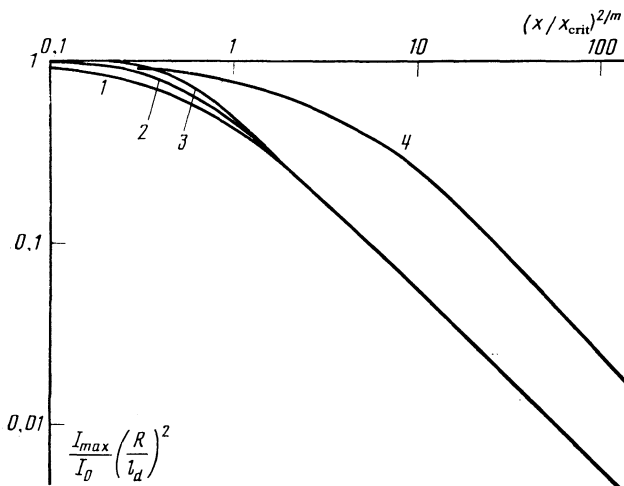


FIG. 3. Maximum intensity on the beam axis as a function of $(x/x_{\text{crit}})^{2/m}$ for nonstationary self-defocusing ($1/\tau = 0$) for different values of m . The aberration-free approximation is shown by curves 1, 2, and 3 for $m = 2, 4,$ and 8, respectively. The numerical solution for $m = 2$ is shown by curve 4. I_0 is the intensity on the beam axis at $z = 0$.

earity of the medium, the shape of the incident radiation pulse, and its amplitude. We note that the variable $x(t)$ enables us to deduce the function $E(t)$ from the solution $A(x)$ of (12) for an arbitrary pulse shape. The coordinate system $\{r, z, x\}$ chosen in this way gives us a set of equations with the single parameter l_d/R .

In the aberration-free approximation (5) for the dimensionless beamwidth $f(z, x)$, we can readily show from (12) that

$$\frac{1}{f} \frac{\partial^2 f}{\partial z^2} - \frac{1}{f^4} \frac{R^2}{l_d^2} = -\frac{m}{2} \frac{R^2}{l_d^2} \int_0^{(\infty)} \frac{dx}{f^{2+m}}. \quad (13)$$

This equation was solved numerically for the following boundary conditions:

$$f(0, x) = 1, \quad \frac{\partial f}{\partial z}(0, x) = -1, \quad f(z, 0) = \left[(1-z)^2 + \frac{z^2 R^2}{l_d^2} \right]^{1/2}.$$

By analogy with the stationary case of defocusing (8), we introduce the critical nonlinearity

$$x_{\text{crit}} = (ka_0)^2 \frac{\delta\epsilon(0, t)}{\epsilon_0} = -\frac{2^{m/2}}{2} \left(\frac{l_d}{R} \right)^{2-m}, \quad (14)$$

where $\delta\epsilon(0, t)$ is the nonlinear increment to the permittivity of the medium in the $z = 0$ plane. For a given pulse shape $\varphi(t)$, the critical self-defocusing energy $\mathcal{E}_{\text{crit}}$ can be determined from x_{crit} . By analogy with the critical power for instantaneous-type self-defocusing, $\mathcal{E}_{\text{crit}}$ is determined by the degree of nonlinearity of the medium and depends on the radiation wavelength and focusing conditions ($m \neq 2$).

Numerical solution of (13) has shown that x_{crit} depends on the defocusing threshold x_{th} [see condition (7)] as follows: $x_{\text{th}} \approx 0.7x_{\text{crit}}$ for $m \geq 2, l_d/R \gg 1$.

In the case of strong defocusing, $x > x_{\text{crit}}$ and broadening of the beam is accompanied by a shift of the nonlinear focus counter to the direction of propagation. Figure 3 shows the maximum light intensity on the axis as a function of $(x/x_{\text{crit}})^{2/m}$ which is linearly related to the total beam energy for $t \gg \tau_p$.

Since for sharp focusing $l_d/R \gg 1$, the interaction is lar-

gely confined to the focal region, and we can choose for the problem parameter combinations such that the solutions are practically independent of l_d/R . Figure 3 and all the subsequent figures are plotted in just these coordinates.

Our numerical calculations have shown that unlike in the instantaneous-type self-defocusing (characterized by saturation of the nonlinear part of the permittivity), in the case of nonstationary self-defocusing the nonlinearity of the medium does not saturate at $x \gg x_{\text{crit}}$ but continues to grow. Figure 4 shows the distribution of $\delta\epsilon$ along the beam axis for different values of x . We note that, in this case ($m = 2$), the distribution $\delta\epsilon(0, z)$ is exactly the same as the axial distribution of the beam energy density inside the medium.

The solution of (13) enables us to determine process parameters such as the nonlinear refractive index and the lateral dimensions of the beam in terms of the integral variable x , whereas the dynamics of the transmitted radiation and its energy characteristics are determined in addition by the shape of the incident pulse $I = I_0 \varphi(t)$. Since the beamwidth on the caustic always increases with time as a result of the accumulation of $\delta\epsilon$, the intensity dynamics in the interior of the medium may be very different from the incident-pulse dynamics, and the pulse may be cut off in the case of strong nonlinearity. The cutoff time t_0 shifts toward lower t as I_0 increases. The most interesting situation is that where cutoff occurs on the leading edge of the pulse and $I(t_0)$ is the peak intensity.

To be specific, let us suppose that the leading edge of the incident pulse is described by $\varphi(t) \sim t^n$. The condition for cutoff on the leading edge of the pulse $\varphi(t)$ is then

$$I + \left(1 + \frac{2}{nm}\right) x \frac{dI}{dx} = 0, \quad (15)$$

where $I = 1/f^2$.

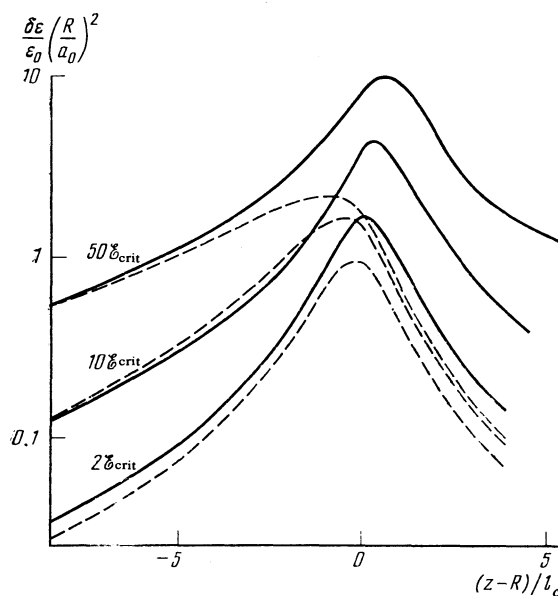


FIG. 4. Distribution of $\delta\epsilon$ on the beam axis in the focal region for nonstationary self-defocusing with $m = 2$ for different values of incident-radiation energy in units of the critical beam energy. Dashed curves correspond to the aberration-free approximation.

Since f is a function of the two variables z and $x(t)$, the pulse dynamics will be different in different z planes. The absolute intensity maximum (maximum with respect to z and t) can be calculated from (15) by using the relationships shown in Fig. 3. Analysis of the solution $f_c(x)$ has shown that, when $n \geq 1$ and $m \geq 2$, condition (15) is satisfied for $x \simeq x_{\text{crit}}$. (We note that, well away from the focal region $z < 1$, the cutoff sets in for $x \gg x_{\text{crit}}$.) Hence, it is readily shown that the peak intensity in the focal region is given by the following function of I_0 :

$$I_{\text{max}} \sim I_0^{(1+mn/2)^{-1}},$$

i.e., nonstationary defocusing does not produce saturation of the light intensity either. By analogy with nonlinear absorption,¹⁴ the rise in intensity in the nonlinear focus during defocusing is determined by the curvature of the leading edge of the incident pulse and the degree of nonlinearity of the medium.

The solution obtained in the aberration-free approximation shows that the accumulation of the nonlinearity in time leads to an asymmetry in the field distribution relative to the focal plane when $\delta\varepsilon/\varepsilon_0 \approx -(a_0/R)^2$ is reached in the medium, and this means that additional beam divergence is produced. It seems to us that the extent to which the strong additional divergence is produced by the medium well beyond the geometric focus cannot be judged from the solution obtained in the axial approximation because it is not clear to what extent the aberration of the induced lens affects wave propagation.

5. NONSTATIONARY SELF-DEFOCUSING. NUMERICAL CALCULATIONS

In view of the foregoing, we have carried out a direct numerical solution of (12). The solution is based on the method proposed in Ref. 8. As in Ref. 8, the system (12) was written in terms of the Lagrange energy coordinates. The fixed grid in Lagrange coordinates is then equivalent to a mobile grid, in Euler coordinates, which is automatically adjusted as the solution develops. This formulation of the problem also enables us to introduce artificial viscosity as a way of combating the resulting nonmonotonic behavior of the phase. When the equation is solved with an integrating-type nonlinearity, the values of the nonlinearity $\delta\varepsilon$ in the two-dimensional $r \times z$ region must be stored for each step in x . The number of points for which the values of $\delta\varepsilon$ were stored was $N_r = 25$ and $N_z = 40$. For points that did not coincide with the nodes of this grid, the values of the nonlinearity were calculated by linear interpolation.

The numerical calculation was performed for $m = 2$ up to $x = 120x_{\text{crit}}$, where x_{crit} is given by (14). As in the case of the instantaneous nonlinearity, inclusion of aberrations for the integrating nonlinearity leads to a much higher value for the defocusing threshold: $x_{\text{th}} = 3.5x_{\text{crit}}$. In contrast to the aberration-free approximation, there was practically no shift of the nonlinear focus in the numerical solution. The dependence of the maximum intensity I_{max} on x was analogous to that obtained in the axial approximation (see Fig. 3), and has the same asymptotic behavior, namely, $I_{\text{max}} \sim 1/x$ for $x \gg x_{\text{crit}}$. This asymptotic behavior shows that the nonlin-

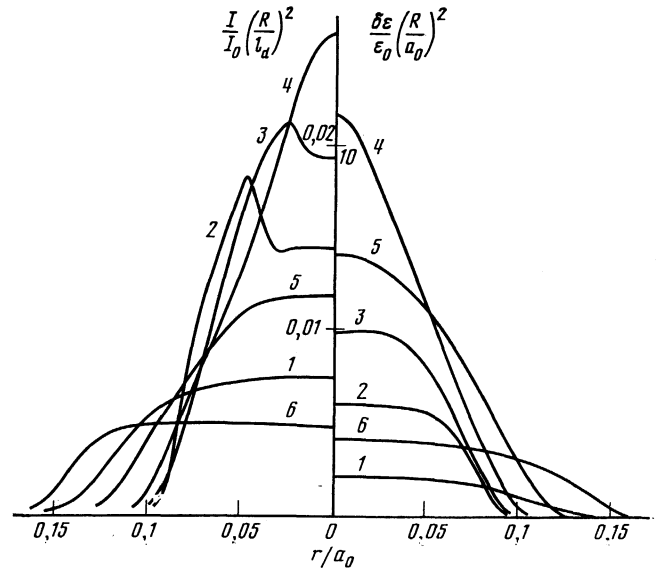


FIG. 5. Radial intensity distribution (left) and nonlinear part of the permittivity ε (right) in different z planes for nonstationary self-defocusing with $m = 2$, $x = 100x_{\text{crit}}$: $R - z = -7.5l_c$ (curve 1); $R - z = -2.9l_c$ (curve 2); $R - z = -1.46l_c$ (curve 3); $z = R$ (curve 4); $R - z = 1.73l_c$ (curve 5), and $R - z = 4l_c$ (curve 6).

earity of the medium does not saturate in the focal region (see Fig. 4)

The operation due to the induced lens can be assessed from Fig. 5, which shows the radial distributions of the light intensity and of the linear part $\delta\varepsilon$ in the difference sections z at $x = 100x_{\text{crit}}$. We note some similarity between the $I(r)$ distributions for nonlinearities of instantaneous and integrating type.

Once the solution $I(r, z, x)$ is available, we can calculate the dynamics of an arbitrary pulse at any point in the nonlinear medium. As an example, consider the point $r = 0$, $z = 1$, which is practically coincident with the nonlinear focus in the case of sharp focusing. Analysis of the numerical solution $I(0, 1, x)$ has shown that if the leading edge of the pulse is described by $\varphi(t) \sim t^n$, the cutoff occurs in this case for $x = 5x_{\text{crit}}$ to $10x_{\text{crit}}$ for any $n \geq 1$. Moreover, the peak intensity in the geometric focus is described by (16), just as in the aberration-free approximation.

When the problem (12) was solved in the aberration-free approximation, it was found that the induced lens and the field distribution relative to the focal plane were both highly asymmetric (cf. Fig. 4). The numerical solution of (12) showed that the beam was, in fact, asymmetric, but the asymmetry was weaker than in the aberration-free approximation. Thus, the increase in the divergence behind the geometric focus ($z = 2$) is twice that for $x \approx 43x_{\text{crit}}$ or $\mathcal{E} = 12.3\mathcal{E}_{\text{th}}$.

We have examined two cases, namely, instantaneous (stationary) and cumulative (integrating) nonlinearity. We have shown that, for an arbitrary nonlinearity that can be described by a power-law formula, the defocusing threshold is determined by $\delta\varepsilon(0, t)$ which depends both on the type of nonlinearity and the shape of the incident pulse. Numerical solution of (1) and (2) in the aberration-free approximation

has shown that, in the presence of relaxation of the nonlinearity, the defocusing threshold is determined by the extremum of the quantity

$$\delta\varepsilon(0, t) = \varepsilon_m E_0^m \exp(-t/\tau) \int_0^t \exp(t'/\tau) \varphi^{m/2}(t') dt'$$

during the pulse. The threshold condition is

$$(ka_0)^2 \frac{\delta\varepsilon(0, t)_{\max}}{\varepsilon_0} = \alpha \left(\frac{l_d}{R} \right)^{2-m} 2^{m/2-1}, \quad \alpha \approx -1,$$

where τ is the nonlinearity relaxation time.

CONCLUSION

Our analysis has thus shown that self-defocusing of sharply-focused beams leads to beam broadening and to a reduction in the intensity in the focal region. Both for stationary and nonstationary defocusing, the maximum change $\delta\varepsilon$ in permittivity does not depend on the frequency of the incident radiation and is determined by the square of the focusing angle ($\delta\varepsilon \sim (a_0/R)^2$). For stationary defocusing, a limitation on $\delta\varepsilon$ leads to intensity saturation in the focal region and to a cutoff in the nonstationary case. In the latter case, the maximum intensity increases with increasing incident power.

Analysis has shown that beam broadening in the case of stationary self-defocusing occurs only near the focal region. It follows that, when the focus lies deep in the nonlinear medium, defocusing cannot be observed by recording changes in the amplitude and phase profile of the transmitted radiation. Defocusing must then be recorded by the interferometric method, using the advance in phase.

On the other hand, additional beam divergence occurs

for nonstationary self-defocusing when $m = 2$. However, experimental detection of this effect for sharp focusing when the focus lies deep inside medium is possible only well above the threshold.

¹¹The focused beam retains its symmetry in the case of Kerr-type self-focusing¹⁰ for beam powers less than the critical value.

¹Yu. P. Raizer, Zh. Eksp. Teor. Fiz. **52**, 470 (1967) [Sov. Phys. JETP **25**, 308 (1967)].

²S. A. Akhmanov, D. P. Krindach, A. P. Sukhorukov, and R. V. Khokhlov, Pis'ma Zh. Eksp. Teor. Fiz. **6**, 509 (1967) [JETP Lett. **6**, 38 (1967)].

³P. J. Kelly, D. S. Ritchie, P. F. Bräunlich, A. Schmid, and F. W. Bryant, IEEE J. Quantum Electron. **QE-17**, 2027 (1981).

⁴D. K. Smit, Proc. IEEE **65**, 59 (1977) [Transl. into Russian].

⁵V. S. Averbakh, A. A. Betin, V. A. Gaponov, *et al.* Izv. Vyssh. Uchebn. Zaved. Radiofiz. **21** 1077 (1978).

⁶S. A. Akhmanov, M. A. Vorontsov, V. P. Kandidov, A. P. Sukhorukov, and S. S. Chesnokov, Izv. Vyssh. Uchebn. Zaved. Radiofiz. **23**, 1 (1980).

⁷S. A. Akhmanov, A. P. Sukhorukov, and R. V. Khokhlov, Usp. Fiz. Nauk **93**, 19 (1967) [Sov. Phys. Usp. **10**, 609 (1968)].

⁸L. M. Degtyarev and V. V. Krylov, Zh. Vychisl. Mat. Mat. Fiz. **17**, 1523 (1977).

⁹A. A. Samarskiĭ and Yu. P. Popov, Raznostnye metody resheniya zadach gazovoi dinamiki (Difference Methods for the Solution of Problems in Gas Dynamics), Nauka, Moscow, 1980.

¹⁰V. N. Lugovoi, Zh. Eksp. Teor. Fiz. **67**, 886 (1973) [Sov. Phys. JETP **38**, 439 (1974)].

¹¹Yu. K. Danileiko, T. P. Lebedeva, A. A. Manenkov, and A. M. Prokhorov, Zh. Eksp. Teor. Fiz. **80**, 487 (1981) [Sov. Phys. JETP **53**, 247 (1981)].

¹²Yu. K. Danileiko, T. P. Lebedeva, A. A. Manenkov, and A. V. Sidorin, Preprint No. 285, FIAN, 1982.

¹³G. A. Askar'yan and M. A. Mukhamadzhano, Pis'ma Zh. Eksp. Teor. Fiz. **33**, 48 (1981) [JETP Lett. **33**, 44 (1981)].

¹⁴Yu. K. Danileiko, T. P. Lebedeva, A. M. Prokhorov, and A. V. Sidorin, Zh. Eksp. Teor. Fiz. **84**, 2032 (1983) [Sov. Phys. JETP **57**, 1183 (1983)].

Translated by S. Chomet